PROGRESS IN COLOR, COLORANTS AND COATINGS

available online @ www.pccc.icrc.ac.ir

Prog. Color Colorants Coat. 8 (2015), 283-294

Ministry of Science, Research and Technology
Institute for Color Science and Technology

Quantum Chemical Studies on Adsorption of Imidazole Derivatives as Corrosion Inhibitors for Mild Steel in 3.5% NaCl Solution

M. Mahdavian*[1], M.M. Attar*[2] and F. Shiran[3]

[1.] Assistant Professor, Surface Coating and Corrosion Department, Institute for Color Science and Technology, P .O. Box 16765-654, Tehran, Iran.

[2.] Professor, Polymer Engineering and Color Technology Department, Amirkabir University of Technology, P. O. Box: 15875-4413, Tehran/Iran.

[3.] a) Lab Analyst, Valoriza Water Australia, Western Australia; b) Southern SeaWater Alliance, Lot 32, Taranto Rd, Binning up, WA, 6233.

ARTICLE INFO

Article history:
Received: 21-06-2015
Final Revised: 20-07-2015
Accepted: 05-09-2015
Available online: 05-09-2015

Keywords:
Adsorption
EIS
Corrosion Inhibitor
Corrosion Product
Quantum Chemistry

ABSTRACT

Adsorption of benzimidazole, 2-methylbenzimidazole and 2-aminobenzimidazole on mild steel in 3.5% NaCl solution was studied using density function theory (DFT) calculations. In this regard, charge transfer resistance (R_{ct}) and double layer capacitance (C_{dl}) obtained by electrochemical impedance spectroscopy (EIS) were used to calculate surface coverage and to build prediction models. When prediction models were only based on quantum chemical parameters of imidazoles, the most effective parameters were frontier orbital energies meaning that dominant mechanism of adsorption was chemisorption. However, models based on imidazoles and iron quantum chemical parameters revealed that the most effective parameter is dipole moment meaning that dominant mechanism of adsorption is physisorption. Prediction models based on inhibitor-$Fe(OH)_2(H_2O)_4$ and inhibitor-$Fe(OH)_3(H_2O)_3$ systems presented dipole moment and electron donating power as the most effective parameters for θR and θC based calculations, respectively. Such a behavior could be attributed to chemical interaction of inhibitors with $Fe(OH)_2(H_2O)_4$ and $Fe(OH)_3(H_2O)_3$ on the mild steel surface resulting in a porous thick layer which could not effectively block the surface but could decrease double layer capacitance. Prog. Color Colorants Coat. 8 (2015), 283-294 © Institute for Color Science and Technology.

1. Introduction

Many studies have been done to evaluate inhibition efficiencies of different inhibitors for a variety of media and substrates. Because of environmental legislation, the use of inhibitors is limited to safe

*Corresponding author: mahdavian-m@icrc.ac.ir and attar@aut.ac.ir

compounds. Most imidazole derivatives are non-toxic and they exhibit a wide variety of pharmacological properties including antitumor activity.

Imidazole derivatives are of particular interest as corrosion inhibitor for Cu, Fe, Zn metal and alloys in acidic media. However, very few investigations have been carried out on corrosion inhibition performance of imidazoles in neutral conditions [1].

Quantum chemistry as a pure computational science has been used by many researchers in corrosion field to evaluate quantum structure–activity relationships (QSAR) of organic inhibitors. Generally, corrosion inhibition efficiency or surface coverage as a function of quantum chemical parameters is studied to build a prediction model. Different methods like weight loss [2, 3], DC polarization [4-6], and EIS [6-10] or average of their combination [11-15] have been used by researches to get valuable information for QSAR studies. Generally, researches consider resistance element or corrosion rate in order to study QSAR.

A glance at recorded capacitance and resistance data in literatures reveals that the obtained surface coverage via capacitance and resistance are not equal in many cases [16-19]. The most frequently used parameters to study QSAR are frontier orbital energies, dipole moment and electronic charge on active sites [20]. However, some authors tend to use other parameters like polarizability, molecular connectivity index, volume and surface area of the molecule, total negative charges, core-core repulsion and binding energy to metal cluster for QSAR study [21-27]. Different calculation techniques have been developed from pure mathematical to semiempirical methods. Density function theory (DFT) method based on Becke's hybrid exchange functional (B3) combined with the LYP correlation functional (B3LYP) has shown the best result and it has been widely used in literatures [28-31]. Linear [32] and non-linear [33, 34] regressions have been used by researchers to find a mathematical models for QSAR study.

The present paper intends to study adsorption of some imidazole derivatives in terms of quantum chemical parameters. In this regard, charge transfer resistance and double layer capacitance extracted from electrochemical measurement are used to evaluate surface coverage of mild steel by imidazoles. Then, the calculated surface coverages are modeled with prediction models based on quantum chemical parameters to study QSAR. In the present study, we chose highest occupied molecular orbital (HOMO) and lowest unoccupied molecular orbital (LUMO) energies, dipole moment and electronic charges at active sites, N1 and N3 according to Figure 1, to evaluate QSAR. Also, non-linear regression was performed to build prediction models.

2. Experimental

2.1. Materials and sample preparation

Synthetic grades of three imidazole derivatives including benzimidazole (BIM), 2-methyl-benzimidazole (MBIM) and 2-aminobenzimidazole (ABIM) were obtained from Merck and used without further purification. Test solutions were prepared in four different concentrations of imidazole derivatives in 3.5% NaCl solution. The concentrations under study were 10^{-2}, 10^{-3}, 10^{-4} and 10^{-5} M.

Mild steel samples were polished with a magnetic polisher to remove mill-scale of the surface, followed by degreasing with xylene and acetone. Surface roughness in the range of 1-5 microns peak-to-valley was measured using Elcometer 223. An area of 1 cm^2 of samples was exposed to the electrolyte whilst other areas of the plates were sealed with beeswax-colophony mixture.

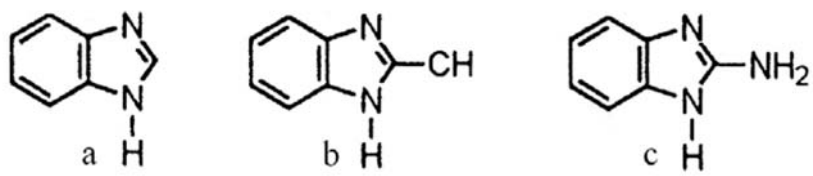

Figure 1: Structure of the studied compounds: (1) BIM, (2) MBIM (3) ABIM.

2.2. Electrochemical impedance spectroscopy measurement

Each specimen was immersed in 100 ml of prepared electrolytes at 30 ºC and electrochemical impedance spectroscopy (EIS) was carried out using Autolab PGSTAT12 after 24 hours immersion. EIS was implemented at open circuit potential in the frequency range of 10^{-2}–10^{+4} Hz with 10 mV perturbation. Reference electrode and counter electrode were silver–silver chloride and platinum (1×1 cm^2), respectively.

2.3. Quantum chemical calculation

Quantum chemical calculations were performed using Gaussian 03W. B3LYP version of DFT was used with 6-311G basis set. Calculations were carried out on a PC computer equipped with AMD Athlon 64 X2 dual core processor 3800 and 1GB RAM. Linear dependency among quantum chemical parameters was studied using NCSS 2007. Also, non-linear regression was performed to build prediction models.

3. Results and Discussion

3.1. Extracted parameters of EIS

All impedance spectra were measured at the respective corrosion potential. The EIS records of this work have been reported in the previous published work [35]. The EIS results were analyzed in terms of the equivalent circuit shown in Figure 2.

Generally, this circuit falls into the classic parallel capacitor and resistor combination. FRA software (version 4.9) of Autolab was used for impedance data analysis. The electrical elements in this figure are R_s, R_{ct} and CPE_{dl} which represent electrolyte resistance, charge transfer resistance at metal electrolyte interface and constant phase element of double layer, respectively. The effective double layer capacitance was calculated according to the following equation [36]:

$$C_{dl} = \frac{(Y_0 . R_{ct})^{1/n}}{R_{ct}} \quad (1)$$

In Eq. 1, C_{dl} represents effective double layer capacitance, Y_0 the magnitude of admittance of CPE, n the exponential term and R_{ct} the charge transfer resistance.

Surface coverage (θ) of the mild steel samples immersed in test electrolytes was calculated by charge transfer resistance (R_{ct}) and double layer capacitance (C_{dl}) according to the following equations.

$$\theta_R = 1 - (\frac{R_{ct,b}}{R_{ct,i}}) \quad (2)$$

$$\theta_C = 1 - (\frac{C_{dl,i}}{C_{dl,b}}) \quad (3)$$

In Eq. 2 and 3, $R_{ct,b}$ and $R_{ct,i}$ are charge transfer resistance of sample immersed in Blank solution and solution containing inhibitor, respectively. Similarly, $C_{dl,b}$ and $C_{dl,i}$ represent double layer capacitance of sample immersed in Blank solution and solution containing inhibitor, respectively. Typical Bode and Nyquist diagrams after fitting with electrical model (Figure 2) are presented in Figure 3a and Figure 3b.

The calculated surface coverages are listed in Table 1. Extended discussion on the extract of circuit elements from EIS data is avoided here as can be found in references [37, 38].

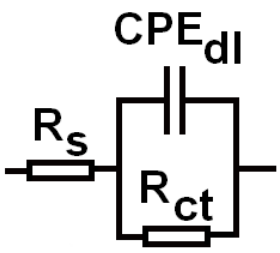

Figure 2: Electrical circuit model used to fit EIS results.

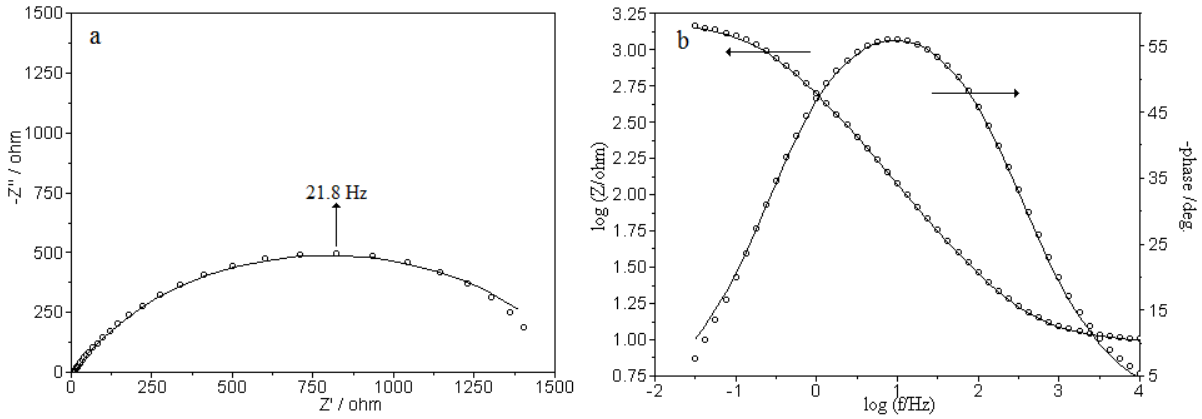

Figure 3: The Nyquist (a) and Bode (b) diagrams resulted from fitting of EIS results for mild steel samples immersed for 1 day at 30ºC in 3.5% NaCl in presence of 0.01 M BIM: Extracted elements from fitting are Rct=1550.9 Ohm.cm2, Y0dl=1.96×10-5 Ω-1.cm-2, ndl=0.711.

Table 1: Surface coverages, θ_R and θ_C, calculated by charge transfer resistance (R_{ct}) and double layer capacitance (C_{dl}) for the different test solutions including: BIM, MBIM, ABIM and Blank.

Test Solutions	Inhibitor Concentration	R_{ct} (Ωcm^2)	C_{dl} (Fcm^{-2})	θ_R(%)	θ_C(%)
BIM	10^{-2} M	1550.9	4.73×10^{-6}	43.38	90.12
	10^{-3} M	1218.1	2.17×10^{-5}	27.91	54.60
	10^{-4} M	1111.0	2.93×10^{-5}	20.96	38.89
	10^{-5} M	947.4	4.36×10^{-5}	7.31	8.99
MBIM	10^{-2} M	1579.4	3.13×10^{-6}	44.40	93.46
	10^{-3} M	1314.4	1.97×10^{-5}	33.19	58.97
	10^{-4} M	1083.4	2.92×10^{-5}	18.95	39.11
	10^{-5} M	987.1	4.20×10^{-5}	11.04	12.37
ABIM	10^{-2} M	1743.8	3.00×10^{-6}	49.64	93.73
	10^{-3} M	1338.1	1.65×10^{-5}	34.37	65.55
	10^{-4} M	1195.7	2.62×10^{-5}	26.56	45.21
	10^{-5} M	1013.9	4.13×10^{-5}	13.39	13.86
Blank	-	878.1	4.79×10^{-5}	-	-

θ_C values are superior to θ_R values as depicted in Table 1. Surface coverage based on resistance represents ability of the adsorbed inhibitors to increase charge transfer resistance and reduce corrosion through surface blocking while surface coverage based on capacitance represents the ability of adsorbed inhibitors to reduce double layer capacity through accumulation on the surface and replacement with water molecules.

It has been reported that inhibition efficiencies calculated by weight loss, polarization or EIS (θ_R) are equal to surface coverage [39-41]. It seems that at least for mild steel immersed in 3.5% NaCl and inhibited by imidazoles, this is not true and more than expected imidazoles are adsorbed on the surface. In other words, for this case study imidazoles are poor blocking agents, despite their adsorption on the surface. Hence, taking inhibition efficiency equal to surface coverage may lead to erroneous results in adsorption isotherm studies.

The big difference between θ_R and θ_C could be related to orientation of inhibitor molecules at the interface and adsorption of the inhibitors on the porous structure of corrosion products. Orientation of inhibitor molecules at the interface is influential on the surface blocking. Imidazoles may adsorb on the surface, but without parallel orientation to the surface they could not serve as effective blocking agents. Similar difference between θ_R and θ_C has been reported in acid solution in the presence of surfactants [42]. On the other hand, according to the Pourbaix diagram of Fe, at neutral condition, corrosion products as ferric and ferrous hydroxides could be formed. Adsorption of the inhibitors on the porous structure of corrosion products may not lead to an efficient surface blocking.

Based on capacitance and resistance values of corroding mild steel at different concentrations of inhibitors, Temkin isotherm (Eq. 4) was found to be the best fitting isotherm. Extended discussion on finding the best fitting isotherm is avoided here as it can be found in references [43-47].

$$\frac{C_{inh}}{55.5}\exp\left(-\frac{\Delta G^0_{ads}}{RT}\right) = \exp(f\theta) \qquad (4)$$

In equation 4, C_{inh} represents the concentration of inhibitor, ΔG^0_{ads} the standard free energy of adsorption, R the universal gas constant, T the absolute temperature, θ the surface coverage and f "surface heterogeneity" parameter. Calculated standard free energy of adsorption and surface heterogeneity parameter corresponding to each imidazole derivative are presented in Table 2.

3.2. Quantum chemical calculations

As surface heterogeneity is included in the prediction models, a mean value should be calculated for the surface heterogeneity parameters listed in Table 2. The harmonic mean values of surface heterogeneity parameters are 8.8 and 20.2 for Temkin isotherms obtained by θ_C and θ_R, respectively.

Before attempt to build prediction models, it needs to be clarified which compound at the mild steel surface could interact with imidazole derivatives. Also, it is quite necessary to determine which quantum chemical parameters and how many quantum chemical parameters could be involved in prediction model.

Ferrous and ferric aqua-hydroxy complexes are probable to exist on Fe surface, according to Pourbiax diagram of iron at neutral pH. Therefore, zero valent Fe, $Fe(OH)_2(H_2O)_4$, $Fe(OH)_3(H_2O)_3$ as possible species are selected for QSAR studies. Frontier orbital energies of iron and its complexes and quantum chemical parameters of imidazole derivatives including frontier orbital energies, dipole moment and charge on possible active adsorption sites (N1 and N3) are presented in Table 3.

Table 2: Standard free energy of adsorption and surface heterogeneity parameter obtained from Temkin isotherm.

Imidazole Derivatives	ΔG^0_{ads} [a] ($KJmol^{-1}$)	ΔG^0_{ads} [b] ($KJmol^{-1}$)	f^a	f^b
BIM	-41.26	-43.07	8.9	20
MBIM	-41.69	-44.04	8.7	20.7
ABIM	-42.61	-45.95	8.9	19.8

[a] The reported items are calculated by capacitance data
[b] The reported items are calculated by resistance data

Table 3: Quantum chemical parameters extracted by DFT/B3LYP/6-311G method for imidazole derivatives and Fe species on the mild steel surface.

Chemical Compound	E_{HOMO}(eV)	E_{LUMO}(eV)	μ (debye)	N1 (charge)	N3 (charge)
BIM	-0.234	-0.025	3.676	-0.800	-0.361
MBIM	-0.229	-0.020	3.695	-0.831	-0.368
ABIM	-0.201	-0.001	4.766	-0.867	-0.411
Fe^0	-0.203	-0.147	-	-	-
$Fe(OH)_3(H_2O)_3$	-0.183	-0.042	-	-	-
$Fe(OH)_2(H_2O)_4$	-0.080	-0.022	-	-	-

The interaction between imidazole derivatives and iron or its corrosion products are defined in terms of electron donating and accepting power. Electron donating power (Don) of an imidazole derivative is inversely proportional to energy difference between HOMO of the imidazole derivative and LUMO of iron species (Eq. 5). The lower the energy difference between the HOMO of the imidazole derivative and the LUMO of iron species, the higher would be the electron donating power and the stronger would be bonding. On the other hand, electron-accepting power (Acc) of an imidazole derivative is inversely proportional to energy difference between HOMO of the iron species and LUMO of the imidazole derivative (Eq. 6). The lower the energy difference between the HOMO of the iron species and the LUMO of the imidazole derivative, the higher would be the electron accepting power which results in stronger back bonding.

$$\text{Don} = \frac{1}{E_{LUMO}\,(\text{iron species}) - E_{HOMO}\,(\text{inhibitor})} \quad (5)$$

$$\text{Acc} = \frac{1}{E_{LUMO}\,(\text{inhibitor}) - E_{HOMO}\,(\text{iron species})} \quad (6)$$

Optimized structures of complex between benzimidazole and $Fe(OH)_2(H_2O)_4$ and benzimidazole and $Fe(OH)_3(H_2O)_3$ are presented in Figure 4. In this figure one water molecule is replaced by one benzoimidazole molecule.

Two different approaches are provided here for QSAR studies which are based on quantum chemical parameters of inhibitor alone and quantum chemical parameters of inhibitor interacting with iron species.

The largest linear independent set of the quantum chemical parameters was evaluated by "Variable Selection for Multivariate Regression" module of NCSS 2007. This module uses McHenry's select algorithm to seek a subset that provides a maximum value of R-Square. This algorithm begins by fitting the full model with all candidate variables. In order to evaluate the model, no linear dependency may exist in the data. A linear dependency occurs when one variable is a weighted average of the rest. For example, if one variable is the total of several others, it cannot be included in the candidate pool.

Initially five quantum chemical parameters including E_{HOMO}, E_{LUMO}, dipole moment and charge on N1 and N3 were considered for QSAR study of inhibitor alone system. The largest possible set of the quantum chemical parameters is based on E_{HOMO}, E_{LUMO} and dipole moment. Incorporation of charge on N1 and N3 in prediction models results in linear dependency. Similarly, five quantum chemical parameters including Don, Acc, dipole moment and charge on N1 and N3 were considered for QSAR study of inhibitor interacting with iron species. The largest possible set of the quantum chemical parameters was based on Don, Acc and dipole moment. Incorporation of charge on N1 and N3 in prediction models resulted in linear dependency. Consequently, two sets of independent three parameters were used to build prediction models. Regarding to two sets of independent three parameters and two set of experimental data (C_{dl} and R_{ct}) to calculate surface coverage (θ_R and θ_C), four combination modes could be considered to build prediction models. These prediction models are presented in Table 4.

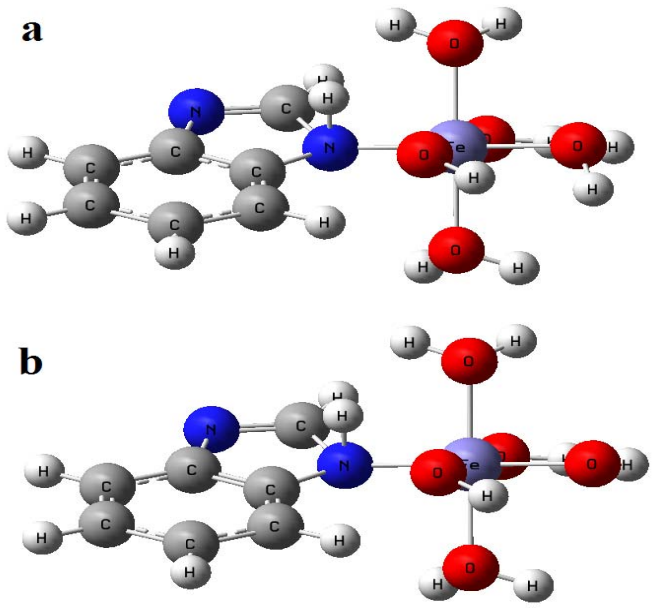

Figure 4: Optimized structure of complex between benzimidazole and $Fe(OH)_2(H_2O)_4$ (a) and the complex between benzimidazole and $Fe(OH)_3(H_2O)_3$ (b).

Table 4: Possible three parametric prediction models based on Temkin isotherm.

inhibitor alone	inhibitor-iron species interaction
$\exp(f.\theta_R) = C_{inh}.(A.E_{HOMO} + B.E_{LUMO} + C.\mu)$	$\exp(f.\theta_R) = C_{inh}.(A.Don + B.Acc + C.\mu)$
$\exp(f.\theta_C) = C_{inh}.(A.E_{HOMO} + B.E_{LUMO} + C.\mu)$	$\exp(f.\theta_C) = C_{inh}.(A.Don + B.Acc + C.\mu)$

The calculated coefficients of the prediction models are listed in Table 5. Also, in Table 5 calculated adsorption free energies and Average Relative Error (ARE) of each model are listed to compare the prediction models. ARE is calculated by Eq. 7.

$$ARE = \frac{1}{n}\sum_{i=1}^{n} \frac{\Delta G^0_{ads}(pre) - \Delta G^0_{ads}(exp)}{\Delta G^0_{ads}(exp)}\Big|_i \qquad (7)$$

In Eq. 7, $\Delta G^0_{ads}(pre)$ represents the standard free energy of adsorption calculated by prediction models, $\Delta G^0_{ads}(exp)$ the standard free energy of adsorption calculated by experimental results and n the number of predicted free energies of each system.

According to Table 5, when inhibitor alone was considered for QSAR calculations, the most effective parameter with θ_R and θ_C based calculations was E_{LUMO}, which has the highest absolute values of coefficients, 1.9×10^7 and 2.8×10^7, compared to E_{HOMO} and μ. Therefore, the value of E_{LUMO} had the greatest impact on inhibition efficiency. In addition, the absolute values of the coefficient of E_{HOMO}, 8.2×10^6 and 8.5×10^6, were higher than μ, 8.2×10^5 and 2.7×10^5, which suggests that chemical interaction of inhibitor with mild steel surface is dominant.

Table 5: The extracted coefficients of the prediction models for surface coverage after linear regression along with predicted standard free energies of adsorption and ARE of each model.

Chemical Compound	Surface coverage based on	A	B	C	ΔG^0_{ads}(pre) ($KJmol^{-1}$) BIM	ΔG^0_{ads}(pre) ($KJmol^{-1}$) MBIM	ΔG^0_{ads}(pre) ($KJmol^{-1}$) ABIM	ARE
inhibitor alone	R_{ct}	8.2×10^6	1.9×10^7	8.2×10^5	-43.72	-44.27	-46.95	0.030238
	C_{dl}	-8.5×10^6	2.8×10^7	-2.0×10^5	-43.43	-43.83	-44.12	
inhibitor & Fe^0	R_{ct}	9.8×10^4	-4.6×10^5	5.7×10^5	-43.79	-44.32	-46.97	0.011743
	C_{dl}	2.5×10^5	3.9×10^5	-1.3×10^6	-41.77	-42.46	-42.38	
inhibitor & $Fe(OH)_3(H_2O)_3$	R_{ct}	1.8×10^5	-5.6×10^5	8.8×10^5	-43.75	-44.29	-46.96	0.009678
	C_{dl}	6.0×10^5	-1.1×10^5	-5.9×10^5	-41.53	-42.30	-42.33	
inhibitor & $Fe(OH)_2(H_2O)_4$	R_{ct}	-3.8×10^5	-1.1×10^5	1.2×10^6	-43.71	-44.25	-46.91	0.014003
	C_{dl}	5.4×10^5	-2.8×10^4	-4.7×10^5	-41.97	-42.65	-42.75	

The influence of dipole moment on corrosion inhibition is not fully understood. Some authors showed increase of dipole moment led to decrease of inhibition and vice versa [48-52]. In order to support the results, a few of these authors claim that lower values of dipole moment will favor accumulation of the inhibitor in the surface layer. In contrast, some authors showed increase of dipole moment led to increase of inhibition and vice versa [53-58], which could be related to dipole-dipole interaction of molecules and metal surface.

Considering all parameters remaining constant, increase of inhibitor dipole moment resulted in increase of θ_R and decrease of θ_C (Table 5a). Distinct impact of dipole moment on θ_R and θ_C could be attributed to their different nature. The value of θ_R is an indication of surface blocking through adsorption of inhibitors. The polar mild steel surface interacts with polar inhibitors, so it seems to be reasonable for higher surface blocking, θ_R, with more polar inhibitors. On the other hand, polarity of the inhibitors affects the dielectric constant so that with increase of dipole moment, the dielectric constant increases. Surface coverage, which is calculated by double layer capacitance decline, is greatly influenced by dielectric constant of the inhibitors replacing water molecules with dielectric constant of 78 [59]. Hence, with increase of dipole moment of inhibitor molecules the calculated surface coverage based on capacitance, θ_C, decreases.

According to Table 5, the prediction models based on quantum chemical parameters of the inhibitors-Fe^0 reveal that the most effective parameter with θ_R and θ_C based calculations is μ, meaning that the major interaction of the molecules with the bare mild steel surface is physical.

The prediction models for surface coverage based on resistance and capacitance values are also listed in Table 5 for $Fe(OH)_2(H_2O)_4$ and $Fe(OH)_3(H_2O)_3$. Dipole moment is the most significant parameter affecting θ_R values, meaning the interaction of inhibitors with corrosion products on mild steel surface is physical when surface coverage is a measure of surface blocking. However, the most significant parameter on θ_C values is electron donating power (Don), which means that the interaction of inhibitors with mild steel surface is chemical when surface coverage is a measure of decrease in double layer capacitance. Such a decline in double layer capacitance could be connected to double layer dielectric constant descent and double layer thickness increase. In the other words, inhibitors could chemically interact with $Fe(OH)_2(H_2O)_4$ and $Fe(OH)_3(H_2O)_3$ on the mild steel surface resulting in a porous thick layer which could not effectively block the surface but could decrease double layer

capacitance. The same impact of dipole moment on θ_R and θ_C as discussed on inhibitor alone and inhibitor-Fe^0 QSAR calculations can be observed for inhibitor-$Fe(OH)_2(H_2O)_4$ and inhibitor-$Fe(OH)_3(H_2O)_3$ QSAR calculations.

Calculated standard free energies of adsorption based on prediction models showed good correlation with standard free energies of adsorption calculated by experimental surface coverage (Table 2). When inhibitor alone was considered for QSAR calculations, the ARE was about 0.0302 while with consideration of recipient side, ARE decreased to below 0.015 which indicated better correlation of standard free energy of adsorption calculated by experimental data and prediction models.

4. Conclusions

The results obtained by quantum chemical calculations on adsorption of imidazole derivatives on mild steel in 3.5 wt. % NaCl solution can be summarized as follow:

1. Inhibition efficiencies calculated by change transfer resistance were generally lower than ones calculated by double layer capacitance. In other words, imidazoles adsorbed more than expected from increase of charge transfer resistance.

2. When prediction models were based on quantum parameters of imidazoles only, the most effective parameter were frontier orbital energies meaning that chemisorption was dominant mechanism of adsorption.

3. Prediction models based on inhibitor-Fe^0 system displayed that the most effective parameter was dipole moment for θ_R and θ_C based calculations, indicating physical interaction as dominant mechanism.

4. Prediction models based on inhibitor-$Fe(OH)_2(H_2O)_4$ and inhibitor-$Fe(OH)_3(H_2O)_3$ systems presented dipole moment and electron donating power as the most effective parameters for θ_R and θ_C based calculations, respectively. Such a behavior could be attributed to chemical interaction of inhibitors with $Fe(OH)_2(H_2O)_4$ and $Fe(OH)_3(H_2O)_3$ on the mild steel surface resulting in a porous thick layer which could not effectively block the surface but could somehow decrease double layer capacitance.

5. The dipole moment showed dual action on prediction models for θ_R and θ_C which could be related to different nature of interactions. Increased polarity of inhibitor molecules affected dipole-dipole interaction of inhibitors with the mild steel surface, which favors more surface blocking, and at the same time results in increased dielectric constant, which causes limited decline in double layer capacitance.

5. References

1. D.Wahyuningrum, S.Achmad, Y. M. Syah, Buchari, B. Bundjali, B. Ariwahjoedi, The Correlation between Structure and Corrosion Inhibition Activity of 4,5-Diphenyl-1-vinylimidazole Derivative Compounds towards Mild Steel in 1% NaCl Solution. *Int. J. Electrochem. Sci.* 3(2008), 154-166.
2. S. Martinez, I. J. Stagljar, Correlation between the molecular structure and the corrosion inhibition efficiency of chestnut tannin in acidic solutions, *Mol. Struct. THEOCHEM,* 640(2003), 167-174.
3. Y. Yan, W. Li, L. Cai, B. Hou, Electrochemical and quantum chemical study of purines as corrosion inhibitors for mild steel in 1 M HCl solution, *Electrochim. Acta,* 53(2008), 5953-5960.
4. K. Bhrara, G.Singh, The inhibition of corrosion of mild steel in 0.5 M sulfuric acid solution in the presence of benzyl triphenyl phosphonium bromide, *Appl. Surf. Sci.*, 253(2006), 846-853.
5. R. Hasanov, M. Sadıkoglu, S. Bilgic, Electrochemical and quantum chemical studies of some Schiff bases on the corrosion of steel in H_2SO_4 solution, *Appl. Surf. Sci.*, 253, 8(2007) 3913-3921.
6. A. A. Rahim, E. Rocca, J. Steinmetz, M. J. Kassim, R. Adnan, M. S. Ibrahim, Mangrove tannins and their flavanoid monomers as alternative steel corrosion inhibitors in acidic medium, *Corros. Sci.* 49(2007), 402-417.
7. P. Zhao, Q. Liang, Y. Li, Electrochemical, SEM/EDS and quantum chemical study of phthalocyanines as corrosion inhibitors for mild

steel in 1 mol/l HCl, *Appl. Surf. Sci.* 252(2005) 1596-1607.

8. S. L Li, Y. G. Wang, S. H. Chen, R. Yu, S. B. Lei, H. Ma, Y. Liu, X. De, Some aspects of quantum chemical calculations for the study of Schiff base corrosion inhibitors on copper in NaCl solutions, *Corros. Sci.,* 41(1999), 1769-1782.
9. M. Lebrini, M. Lagrenee, M. Traisnel, L. Gengembre, H. Vezin, F. Bentiss, Enhanced corrosion resistance of mild steel in normal sulfuric acid medium by 2,5-bis(n-thienyl)-1,3,4-thiadiazoles: Electrochemical, X-ray photoelectron spectroscopy and theoretical studies, *Appl. Surf. Sci.* 253(2007), 9267.
10. M. Lebrini, M. Traisnel, M. Lagrenee, B. Mernari, F. Bentiss, Inhibitive properties, adsorption and a theoretical study of 3,5-bis(n-pyridyl)-4-amino-1,2,4-triazoles as corrosion inhibitors for mild steel in perchloric acid, *Corros. Sci.* 50(2008), 473-479.
11. M. Lebrini, M. Lagrenee, H. Vezin, L. Gengembre, F. Bentiss, Electrochemical and quantum chemical studies of new thiadiazole derivatives adsorption on mild steel in normal hydrochloric acid medium, Corros. Sci. 47 (2005) 485-505.
12. E. S. H. El Ashry, A. El Nemr, , S. A. Esawy, S. Ragab, Corrosion inhibitors: Part II: Quantum chemical studies on the corrosion inhibitions of steel in acidic medium by some triazole, oxadiazole and thiadiazole derivatives, *Electrochim. Acta,* 51(2006), 3957.
13. K. F. Khaled, Experimental and theoretical study for corrosion inhibition of mild steel in hydrochloric acid solution by some new hydrazine carbodithioic acid derivatives, *Appl. Surf. Sci.* 252(2006), 4120-4128.
14. H. Ashassi-Sorkhabi, B. Shaabani, D. Seifzadeh, Effect of some pyrimidinic Shciff bases on the corrosion of mild steel in hydrochloric acid solution, *Electrochim. Acta* 50(2005), 3446-3452.
15. E. Machnikova, K. H. Whitmire, N. Hackerman, Corrosion inhibition of carbon steel in hydrochloric acid by furan derivatives, *Electrochim. Acta,* 53(2008), 6024-6032.
16. A. Khavasfar, M. H. Moayed, M.M. Attar, An Investigation on the performance of an imidazoline based commercial Corrosion inhibitor on CO_2 corrosion of gas-well tubing steel by EIS technique, Iranian J. Mater. Sci. Eng. 4(2007), 1-8.
17. N. Huynh, S. E. Bottle, T. Notoya, A. Trueman, B. Hinton and D. P. Schweinsberg, Studies on alkyl esters of carboxybenzotriazole as inhibitors for copper corrosion, *Corros. Sci.* 44(2002), 1257-1276.
18. S. A. Ali, H. A. Al-Muallem, M. T. Saeed, S. U. Rahman, Hydrophobic-tailed bicyclo-isoxazolidines: A comparative study of the newly synthesized compounds on the inhibition of mild steel corrosion in hydrochloric and sulfuric acid media*, Corros. Sci.* 50(2008), 664-675.
19. R. A. Prabhu, T. V. Venkatesha, A. V. Shanbhag, B. M. Praveen, G. M. Kulkarni, R. G. Kalkhambkar, Quinol-2-thione compounds as corrosion inhibitors for mild steel in acid solution, *Mater. Chem. Phys.* 108(2008), 283-289.
20. D. Q. Zhang, Z. X. An, Q. Y. Pan, L. X. Gao, G. D. Zhou, Comparative study of bis-piperidiniummethyl-urea and mono-piperidiniummethyl-urea as volatile corrosion inhibitors for mild steel, *Corros. Sci.* 48(2006), 1437-1448.
21. S. G. Zhang, W. Lei, , M. Z. Xia, F. Y. Wang, QSAR study on N-containing corrosion inhibitors: Quantum chemical approach assisted by topological index, *J. Mol. Struct. THEOCHEM,* 732(2005), 173-182.
22. J. H. Henriquez-Romana, L. Padilla-Campos, M. A. Paez, J. H. Zagal, M. A. Rubio, C. M. Rangel, J. Costamagnaa,. G.Cardenas-Jiron, The influence of aniline and its derivatives on the corrosion behaviour of copper in acid solution: a theoretical approach, *J. Mol. Struct. THEOCHEM,* 757(2005), 1-7.
23. M. Lashkari, M. R. Arshadi, DFT studies of pyridine corrosion inhibitors in electrical double layer: solvent, substrate, and electric field effects, *Chem. Phys.* 299 (2004), 131-137.
24. M. R. Arshadi, M. Lashkari, Gh. Parsafar, A., Cluster approach to corrosion inhibition problems: interaction studies, *Mater. Chem. Phys.* 86 (2004), 311-314.
25. F. Bentiss, M.Traisnel, , H. Vezin, H. F.

Hildebrand, M. Lagrenee, 2,5-Bis(4-dimethylaminophenyl)-1,3,4-oxadiazole and 2,5-bis(4-dimethylaminophenyl)-1,3,4-thiadiazole as corrosion inhibitors for mild steel in acidic media, *Corros. Sci.* 46(2004), 2781-2792.

26. F. Bentiss, M. Lebrini, H. Vezin, M. Lagrenee, Experimental and theoretical study of 3-pyridyl-substituted 1,2,4-thiadiazole and 1,3,4-thiadiazole as corrosion inhibitors of mild steel in acidic media, *Mater. Chem. Phys*. 87(2004) 18-23.
27. M. Ozcan, I. Dehri, M. Erbil, Organic sulphur-containing compounds as corrosion inhibitors for mild steel in acidic media: correlation between inhibition efficiency and chemical structure, *Appl. Surf. Sci.* 236(2004), 155-164.
28. F.A. Carey, R. J. Sundberg, Advanced Organic Chemistry, fifth ed., Springer, 2007.
29. R. J. Gillespie, P. L. A. Popelier, Chemical Bonding and Molecular Geometry, Oxford University Press, 2001.
30. Weinhold, F. and Landis, C.R. Valency and Bonding: A Natural Bond Orbital Donor–Acceptor Perspective, Cambridge University Press, 2005.
31. P. S. Hill, E. A. Schauble, Geochim. Cosmochim. Acta 72/8 (2008) 1939.
32. G. Bereket, C. Ogretir, C. Ozsahin, , Quantum chemical studies on the inhibition efficiencies of some piperazine derivatives for the corrosion of steel in acidic medium, *J. Mol. Struct. THEOCHEM,* 663(2003), 39-46.
33. H. Ashassi-Sorkhabi, B.Shaabani, D. Seifzadeh, , Corrosion inhibition of mild steel by some schiff base compounds in hydrochloric acid, *Appl. Surf. Sci.* 239(2005), 154-164.
34. I. Lukovits, I. Bako, A. Shaban, E. Kalman, Polynomial model of the inhibition mechanism of thiourea derivatives, *Electrochim. Acta,* 43(1998), 131-136.
35. M. Mahdavian, M. M. Attar, Electrochemical assessment of imidazole derivatives as corrosion inhibitors for mild steel in 3.5% NaCl solution, *Prog. Color Colorants Coat.,*8(2015), 177-196.
36. B. Hirschorn, M. E. Orazem, B. Tribollet, V. Vivier, I. Frateur, M. Musiani, Determination of effective capacitance and film thickness from constant phase-element parameters, *Electrochimica Acta,* 55(2010), 6218-6227.
37. S. M. Amoozadeh, J. Mahdavian, Synergistic inhibition effect of Zinc acethylacetonate and benzothiazole in epoxy coating on the corrosion of mild steel,. Mater Eng Performance, 24(2015) 2464-2472.
38. E. Alibakhshia, E. Ghasemi, M. Mahdavian, Optimization of potassium zinc phosphate anticorrosion pigment by Taguchi experimental design, *Prog Org Coat,* 76(2013), 224-230.
39. X. Li, L. Tang, G. Mu, L. Li G. Liu, The synergistic inhibition of the cold rolled steel Corrosion in 0.5 M sulfuric acid by the mixture of OP and bromide ion*, Mater. Lett.* 61(2007), 2723-2727.
40. H. Amar, J. Benzakour, A. Derja, D. Villemin, B. Moreau, T. Braisaz, Piperidin-1-yl-phosphonic acid and (4-phosphono-piperazin-1-yl) phosphonic acid: A new class of iron corrosion inhibitors in sodium chloride 3% media, *Appl. Surf. Sci.* 252(2006), 6162-6172.
41. G. K. Gomma, Effect of azole compounds on corrosion of copper in acid medium, *Mater. Chem. Phys.* 56(1998), 27-34.
42. M. Motamedi, A. R. Tehrani-Bagh, M. Mahdavian, Effect of aging time on corrosion inhibition of cationic surfactant on mild steel in sulfamic acid cleaning solution, *Corros. Sci*. 70(2013), 46-54.
43. A. Y. El-Etre, Inhibition of C-steel corrosion in acidic solution using the aqueous extract of zallouh root, *Mater. Chem. Phys.* 108(2008), 278-282.
44. A. Ghanbari, M. M. Attar, M. Mahdavian, Corrosion inhibition performance of three imidazole derivatives on mild steel in 1 M phosphoric acid, *Mater Chem Phys*, 124(2010), 1205-1209.
45. M. Motamedi, A. R. Tehran-bagha, M. Mahdavian, A comparative study on the electrochemical behavior of mild steel in sulfamic acid solution in the presence of monomeric and gemini surfactants*, Electrochim. Acta,* 58(2011), 488-496.
46. M. N. H. Moussa, A. A. El-Far, A. A. El-Shafei, The use of water-soluble hydrazones as inhibitors for the corrosion of C-steel in acidic medium, *Mater. Chem. Phys*. 105(2007), 105-113.

47. E. E. Oguzie, Corrosion inhibition of aluminium in acidic and alkaline media by Sansevieria trifasciata extract, *Corros. Sci.* 49(2007), 1527-1539.
48. K. F. Khaled, Molecular simulation, quantum chemical calculations and electrochemical studies for inhibition of mild steel by triazoles, *Electrochim. Acta*, 53(2008), 3484-3492.
49. F. Bentiss, M. Lebrini, M. Lagrenee, M. Traisnel, A. Elfarouk, H. Vezin, The influence of some new 2,5-disubstituted 1,3,4-thiadiazoles on the corrosion behaviour of mild steel in 1 M HCl solution: AC impedance study and theoretical approach, *Electrochim. Acta*, 52(2007), 6865-6872.
50. M. Lebrini, M. Lagrenee, H. Vezin, L. Gengembre, F. Bentiss, Electrochemical and quantum chemical studies of new thiadiazole derivatives adsorption on mild steel in normal hydrochloric acid medium, *Corros. Sci.* 47(2005), 485-505.
51. N. Khalil, Quantum chemical approach of corrosion inhibition, *Electrochim. Acta*, 48(2003), 2635-2640.
52. F. Bentiss, M. Traisnel, H. Vezin, M. Lagrenee, Linear resistance model of the inhibition mechanism of steel in HCl by triazole and oxadiazole derivatives: structure–activity correlations*, Corros. Sci.* 45(2003), 371-380.
53. E. S. H. El Ashry, A. El-Nemr, S. A. Essawy, S.Ragab, Corrosion inhibitors part V: QSAR of benzimidazole and 2-substituted derivatives as corrosion inhibitors by using the quantum chemical parameters, *Prog. Org. Coat.* 61(2008), 11-20.
54. M. Lebrini, M. Lagrenee, H. Vezin, M. Traisnel, F. Bentiss, Experimental and theoretical study for corrosion inhibition of mild steel in normal hydrochloric acid solution by some new macrocyclic polyether compounds, *Corros. Sci.* 49(2007), 2254-2269.
55. R. Hasanov, M. Sadıkoglu, S. Bilgic, Electrochemical and quantum chemical studies of some Schiff bases on the corrosion of steel in H2SO4 solution, *Appl. Surf. Sci.* 253(2007), 3913-3921.
56. A.Yurt, S. Ulutas, H. Dal, Electrochemical and theoretical investigation on the corrosion of aluminium in acidic solution containing some Schiff bases, *Appl. Surf. Sci.* 253 (2006), 919-925.
57. S. G. Zhang, W. Lei, M. Z. Xia, F. Y. Wang, QSAR study on N-containing corrosion inhibitors: Quantum chemical approach assisted by topological index, *J. Mol. Struct. THEOCHEM,* 732(2005), 173-182.
58. K. F. Khaled, K. Babic-Samardzija, N. Hackerman, Theoretical study of the structural effects of polymethylene amines on corrosion inhibition of iron in acid solutions, *Electrochim. Acta*, 50(2005), 2515-2520.
59. J. O'M Bockris, A. K. N.Reddy, Modern Electrochemistry: An Introduction to an Interdisciplinary Area, Springer, 1973.